INFECTION AND IMMUNITY, Oct. 2002, p. 5381–5389 Vol. 70, No. 10
0019-9567/02/$04.00+0 DOI: 10.1128/IAI.70.10.5381–5389.2002

Contribution of Membrane-Damaging Toxins to *Bacillus* Endophthalmitis Pathogenesis

Michelle C. Callegan,[1,2,3]* Daniel C. Cochran,[1,3] Scott T. Kane,[1,3] Michael S. Gilmore,[1,2,3] Myriam Gominet,[4] and Didier Lereclus[4]

Department of Ophthalmology[1] and Department of Microbiology and Immunology,[2] University of Oklahoma Health Sciences Center, and Molecular Pathogenesis of Eye Infections Research Center, Dean A. McGee Eye Institute,[3] Oklahoma City, Oklahoma, and Unité de Biochimie Microbienne, Institut Pasteur, Paris cedex, France[4]

Received 8 April 2002/Returned for modification 22 May 2002/Accepted 2 June 2002

Membrane-damaging toxins are thought to be responsible for the explosive clinical course of *Bacillus* endophthalmitis. This study analyzed the contribution of phosphatidylinositol-specific phospholipase C (PI-PLC) and phosphatidylcholine-specific phospholipase C (PC-PLC) to the pathogenesis of experimental *Bacillus* endophthalmitis. Isogenic mutants were constructed by insertion of *lacZ* into *Bacillus thuringiensis* genes encoding PI-PLC (*plcA*) and PC-PLC (*plcB*). Rabbit eyes were injected intravitreally with 2 $\log_{10}$ CFU of strain BT407 (wild type), the PI-PLC mutant (BT*plcA*::*lacZ*), or the PC-PLC mutant (BT*plcB*::*lacZ*). The rates of decrease in retinal responses of eyes infected with the isogenic mutants were similar to that of wild type, with all infections resulting in elimination of retinal function by 18 h. Strain BT407 caused a significant increase in the latency of retinal responses at 6 h, but strains BT*plcA*::*lacZ* and BT*plcB*::*lacZ* did not. All strains elicited significant inflammatory cell influx into the anterior chamber by 12 h. Histologically, eyes infected with each strain were indistinguishable throughout the infection course. In this model, neither PI-PLC nor PC-PLC had an effect on the course or severity of experimental *Bacillus* endophthalmitis. Alterations in retinal responses early in infection may mark the beginnings of specific photoreceptor or glial cell dysfunction.

The most severe form of intraocular bacterial infection (endophthalmitis) is caused by *Bacillus* spp. *Bacillus cereus*, in particular, causes a uniquely explosive intraocular infection that can result in significant vision loss, and frequently loss of the eye itself, within 1 to 2 days (10). *Bacillus* endophthalmitis typically results from penetrating trauma of the globe with a contaminated foreign body but can also result from metastatic spread of organisms to the eye following bacteremia in the immunocompromised. Despite aggressive antibiotic, anti-inflammatory, and surgical intervention, the disease course is frequently rapid and destructive, highlighting the limitations of present therapeutic strategies.

The unique virulence of *B. cereus* endophthalmitis is typically ascribed to toxins produced by the organism in the eye during infection. Membrane-damaging toxins such as *Staphylococcus aureus* alpha-toxin (9, 10), *Enterococcus faecalis* cytolysin (22), and *Streptococcus pneumoniae* pneumolysin (34) have been identified as virulence factors in ocular infection. *B. cereus* secretes a number of factors that may contribute to disease pathogenicity, namely, hemolysins, lipases, enterotoxins, and proteases (14). Our analysis of the contribution of one toxin, hemolysin BL, to the course and severity of experimental endophthalmitis demonstrated that this enterotoxin contributed little to the intraocular virulence of *B. cereus* (11). Both the wild type and an isogenic hemolysin BL-deficient mutant resulted in the destruction of retinal architecture, complete loss of retinal function, and significant intraocular inflammation within 12 h (11).

A number of other *B. cereus* toxins are potential intraocular virulence factor candidates. Phosphatidylcholine-phospholipase C (PC-PLC) and sphingomyelinase (SPH), which comprise the cytolytic unit cereolysin AB, could be potential virulence factors because of the combined activities of these components against mammalian cells (15). Like cereolysin AB, the alpha-toxin of *Clostridium perfringens* possesses PC-PLC and SPH activities and is a key virulence factor in both gas gangrene and food-borne illness (2, 39). PC-PLC is necessary for cell-to-cell spread of invasive *Listeria monocytogenes* infection (41). The SPH activity of staphylococcal beta-toxin contributes only minimally to the virulence of *S. aureus* endophthalmitis (10) and keratitis (35) but is a known inducer of apoptosis in mammalian cells (17, 45). The intraocular toxicity of *B. cereus* PC-PLC and SPH has been analyzed. Purified PC-PLC was toxic to retinal buttons in vitro and to the retina in vivo, whereas purified SPH was minimally toxic in vitro (4). A third toxin, phosphotidylinositol-phospholipase C (PI-PLC), has been suggested to be a virulence factor for *L. monocytogenes* (38, 43) and *S. aureus* (12, 29) but has been shown to be minimally toxic to retinal buttons in vitro (4).

This study addressed the contribution of PC-PLC and PI-PLC to the pathogenesis of experimental endophthalmitis by using *B. thuringiensis* as the test organism. *B. thuringiensis* is a spore-forming soil entomopathogenic organism that is used widely as an organic pesticide and whose genomic and phenotypic profile is very closely related to, and in some cases over-

* Corresponding author. Mailing address: Department of Ophthalmology DMEI 418, 608 Stanton L. Young Blvd., Oklahoma City, OK 73104. Phone: (405) 271-1084. Fax: (405) 271-8781. E-mail: michelle-callegan@ouhsc.edu.

TABLE 1. Bacterial strains and plasmids used in this study

Strain or plasmid	Relevant properties	Reference or source
Strains		
BT407	Wild-type *B. thuringiensis*, Cry$^-$	27
BT*plcA*::*lacZ*	BT407 with *lacZ* insertion into *plcA*	This work
BT*plcB*::*lacZ*	BT407 with *lacZ* insertion into *plcB*	This work
E. coli TG1	[Δ(*lac-proAB*) *supE thi hdsD5* (F′ *traD36 proA*$^+$ *proB*$^+$ *lacI*^{q}ZΔM15)]	16
E. coli SCS110	[*rpsL thr leu endA thi-1 lacY galK galT ara tonA tsx dam dcm supE44* Δ(*lac-proAB*) (F′ *traD36 proAB lacI*^{q}ZΔM15)]	16
Plasmids		
pHT304-18Z	Source of promotorless *lacZ* for insertional mutagenesis of BT407	1
pRN1501	Temperature-sensitive vector containing the *ori*(Ts) and *erm* of pE194ts and the *ori*Ec, *amp*, and multicloning region of pBR322	28, 44

TABLE 2. PCR primers used in this study

Primer	Sequence[a]	Restriction site
PlcA1	5′-GTAGATACAACTACAGCTGAAC	
PlcA2	5′-GCTCTAGACACTTTTTCTGTTTTTACATC	*Xba*I
PlcA3	5′-GTATGGGGAATGACGCAAG	
PlcA4	5′-GCGGATCCTTGAATTCCCAGCCTACTC	*Bam*HI
PlcB1	5′-CCCAAGCTTGTTTAGATAAGCCTTAATAATAGT	*Hin*dIII
PlcB2	5′-CGGAATTCCATTGTCTGGATCATAGAAATG	*Eco*RI
PlcB3	5′-CGGAATTCCATTTGCAAAGCAGGCAAAAG	*Eco*RI
PlcB4	5′-CGGGATCCGTACGTATCAAACCAAAGC	*Bam*HI
LacZ-F	5′-GGTTAAATTGCCAACGCTTAATTAAC	
LacZ-R	5′-GTTATCTGGAAGATCAGGATATGTGG	

[a] The restriction site is underlined.

laps, that of *B. cereus* (18). Because systems for genetic manipulation of *B. thuringiensis* have been developed (27), this organism was used in the present studies. *B. thuringiensis* wild type and isogenic PC-PLC or PI-PLC mutants were analyzed in a highly sensitive in vivo model to define their contributions to the evolution of endophthalmitis.

MATERIALS AND METHODS

Bacterial strains and plasmids. The wild-type *B. thuringiensis* strain used in these studies (BT407) has been cured of the plasmid encoding the insecticidal crystalline toxin (Cry$^-$) (27) but produces several of the same toxins as *B. cereus*. Construction of isogenic mutants of strain BT407 specifically deficient in PI-PLC or PC-PLC is described below. The use of *E. coli* strains SCS110 and TG1 for plasmid construction and cloning, respectively, has been described previously (16). Bacterial strain and plasmid profiles are summarized in Table 1.

Culture media and reagents. For mutant strain construction, *Escherichia coli* and *B. thuringiensis* were cultured in Luria-Bertani medium with or without antibiotic selection as appropriate. Antibiotics used for transformant selection included erythromycin (25 μg/ml) and ampicillin (100 μg/ml). For phenotypic analysis of bacterial culture supernatants and inoculum preparation, *B. thuringiensis* was cultured in brain heart infusion (BHI [Difco, Detroit, Mich.]). All reagents used in phenotypic assays were purchased from Sigma (St. Louis, Mo.) unless otherwise specified.

DNA techniques. Extraction of plasmid DNA from *E. coli* and chromosomal DNA from *B. thuringiensis* and DNA fragment digestions, purifications, and ligations were performed essentially as described previously (30). Restriction enzymes and T4 DNA ligase were used as recommended by the manufacturers. Primers used for PCR amplification of *plcA* and *plcB* were synthesized by Genset (Paris, France) and Integrated DNA Technologies (Coralville, Iowa). Primers used for PCR amplification of *lacZ* were synthesized by Integrated DNA Technologies.

Generation of isogenic *B. thuringiensis* mutants. The PI-PLC isogenic mutant (designated BT*plcA*::*lacZ*) was created by disruption of the PI-PLC *plcA* gene of strain BT407 with a promoterless *lacZ* gene into the 5′ part of the coding sequence. A DNA region just upstream from the *plcA* coding sequence and an internal region of *plcA* were amplified by PCR using primers PlcA1 and PlcA2 and primers PlcA3 and PlcA4, respectively (Table 2). Primer sequences were selected from the published nucleotide sequence of *B. cereus plcA* (accession no. M30809 [24]). Amplified DNA fragments were digested with appropriate restriction enzymes and inserted separately into pUC18. The promoterless *lacZ* gene was purified as a 3.2-kb *Xba*I-*Eco*RI DNA fragment from pHT304-18Z (1). The upstream and internal parts of the *plcA* gene were purified as *Hin*dIII-*Xba*I and *Eco*RI-*Bam*HI fragments, respectively, and ligated with the *lacZ* gene between the *Hin*dIII and *Bam*HI sites of the thermosensitive plasmid pRN5101 (28, 44). The ligation mixture was then used to transform *E. coli* to ampicillin resistance. The plasmid isolated from the transformants was verified by restriction mapping. This recombinant plasmid was introduced into strain BT407 by electroporation as previously described (27). Transformants were resistant to erythromycin and had a blue phenotype (Lac$^+$) on Luria-Bertani plates containing 5-bromo-4-chloro-3-indolyl-β-D-galactopyranoxide (X-Gal) (40 μg/ml; Sigma). The chromosomal wild-type copy of *plcA* was replaced with the disrupted copy by homologous recombination as previously described (25). In the resulting *B. thuringiensis* recombinant strain, the *lacZ* gene was transcribed from the *plcA* promoter and was thus controlled by the transcriptional activator PlcR (26).

The PC-PLC isogenic mutant (designated BT*plcB*::*lacZ*) was created by disruption of the PC-PLC *plcB* gene of strain BT407 with a promoterless *lacZ* gene, as described above. Regions corresponding to the 5′ and 3′ ends of *plcB* were amplified by PCR from the chromosomal DNA of strain BT407, using primers PlcB1 and PlcB2 and primers PlcB3 and PlcB4, respectively (Table 2). The sequences of these primers were selected from published sequences of the *B. cereus* PC-PLC gene (accession no. X12854 [23]). The promoterless *lacZ* gene was purified as a 3.2-kb *Eco*RI-*Eco*RI DNA fragment from pHT304-18Z (1). The 5′ and 3′ regions of *plcB* were purified as *Hin*dIII-*Eco*RI and *Eco*RI-*Bam*HI fragments, respectively, and ligated with the *lacZ* gene between the *Hin*dIII and *Bam*III sites of pRN5101 (28, 44). The orientation of *lacZ* was confirmed by restriction mapping, and plasmids carrying *lacZ* transcribed in the same direction as *plcB* were selected. These recombinant plasmids were introduced into strain BT407 by electroporation, and the chromosomal wild-type copy of *plcB* was replaced with the disrupted copies by homologous recombination as previously described (25).

PCR amplification of *plcA*, *plcB*, and *lacZ*. The presence of *plcA*, *plcB*, and *lacZ* in the genomes of *B. thuringiensis* wild type and isogenic mutants was confirmed by PCR using primers PlcA1 and PlcA4 (*plcA*), PlcB1 and PlcB4 (*plcB*), or LacZ-F and LacZ-R (*lacZ*), respectively (Table 2). *B. thuringiensis* chromosomal DNA was isolated by phenol-chloroform extraction. PCR mixtures of 10 μl contained 0.25 to 1.0 μg of genomic DNA, 0.25 mM each deoxynucleoside triphosphate, TaKaRa DNA polymerase buffer (10× supplemented with 25 mM $MgCl_2$ [final concentration, 2.5 mM $MgCl_2$]; PanVera Corp., Madison, Wis.), 0.2 to 1.0 mM each primer, depending on the primer set used, and 0.025 U of TaKaRa *Taq* polymerase (PanVera). PCR fragments were amplified from *B. thuringiensis* BT407 genomic DNA under the following conditions: 30 cycles of 94°C for 1 min, 62°C (*plcA*) or 63°C (*plcB*) for 1 min, and 72°C for 1 min, followed by one 10-min elongation at 72°C. PCR fragments were amplified from the genomic DNA of strains BT*plcA*::*lacZ* and BT*plcB*::*lacZ* under the following conditions: 30 cycles of 94°C for 1 min, 57°C (*plcA*) or 63°C (*plcB*) for 1 min, and 72°C for 3 min 30 s, followed by one 10-min elongation at 72°C. *lacZ* fragments were amplified from the genomic DNA of all strains under the following conditions: 30 cycles of 94°C for 1 min, 55°C for 1 min, and 72°C for 1 min, followed by one 10-min elongation at 72°C. Amplified fragments were resolved on a 0.8% agarose gel.

Phenotypic analysis of *Bacillus* strains. (i) Hemolytic activity. Hemolytic activity was determined by quantifying hemoglobin release from sheep and rabbit erythrocytes. Briefly, twofold serial dilutions of filtered logarithmic-phase (8-h) and stationary-phase (18-h) culture supernatants were incubated with an equal volume of 4% (vol/vol) sheep or rabbit erythrocytes (Rockland Inc., Gilbertsville, Pa.) in phosphate-buffered saline. Following a 30-min incubation at 37°C, the optical density at 540 nm (OD_{540}) was measured. The hemolytic titer was determined as the dilution of supernatant exhibiting 50% hemolysis. The hemolytic

activity of individual colonies was also analyzed on BHI agar supplemented with 5% sheep or rabbit erythrocytes.

(ii) Proteolytic activity. Proteolytic activity was determined on hide azure powder (Sigma). Briefly, filtered 10-h culture supenatants were incubated with 10 mg of hide azure powder in assay buffer (10 mM Tris HCl, 10 mM $CaCl_2$ [pH 8.0]) for 2 h and the OD_{562} was measured (37). Proteolytic activity is expressed in units per milliliter. The proteolytic activity of individual colonies was also analyzed on BHI agar supplemented with 2.5% skim milk (Difco).

(iii) PI-PLC activity. PI-PLC activity in culture supernatants was measured by a colorimetric microtiter assay adapted from that described by Ikezawa and Taguchi (20). *B. cereus* PI-PLC standards (Sigma), filtered 10-h culture supernatants, and heat-denatured standards and supernatant controls were serially diluted 1:2 in isotonic phosphate buffer (150 mM NaCl in 5 mM sodium phosphate buffer [pH 7.6]). The 50-μl volumes of PI-PLC standards or culture supernatants were added to 950 μl of bovine erythrocyte ghosts (10% [vol/vol] in isotonic phosphate buffer), and the suspensions were incubated for 30 min at 37°C. The suspensions were centrifuged at 16,000 × *g* to pellet the cell debris. A 25-μl volume of supernatant was transferred to microtiter wells, to which 200 μl of 100 mM sodium phosphate buffer (pH 7.5), 12.5 μl of 5,5′-dithio-bis(2-nitrobenzoic acid) (DTNB) (10 mM in sodium phosphate buffer), and 12.5 μl of acetylthiocholine (12.5 mM in sodium phosphate buffer) were added. Following a 4-h vacuum incubation at room temperature, the OD_{405} was determined. PI-PLC concentrations in culture supernatants were extrapolated from the *B. cereus* PI-PLC standard curve. Each sample and standard were assayed in triplicate.

(iv) PC-PLC activity. PC-PLC activities in culture supernatants were measured by an egg yolk agar well diffusion assay adapted from that described by Gilmore et al. (15). *B. cereus* PC-PLC standards and filtered 8-h culture supernatants were serially diluted 1:2 in dilution buffer (0.5 M Tris-HCl, 2 mM $ZnCl_2$). Then 7-mm wells were punched into BHI agar supplemented with 5% egg yolk enrichment (ICN Biomedicals Inc., Aurora, Ohio); a 50-μl standard or supernatant was added to each well. Following a 5-h incubation at 37°C, turbidity zone diameters were measured. PC-PLC concentrations in culture supernatants were extrapolated from the *B. cereus* PC-PLC standard curve. Each sample and standard was assayed in triplicate.

(v) SPH assay. SPH activities in culture supernatants were measured by a colorimetric microtiter assay adapted from that described by Gatt et al. (13). *B. cereus* SPH standards (Sigma) and filtered 4-, 8-, 10-, 12-, and 18-h culture supernatants were diluted with an equal volume of assay buffer (125 mM Tris-Cl, 25 mg of $MgCl_2$ per ml, 0.5% Triton X-100, 50% BHI [pH 7.4]). The trinitrophenylaminolauroyl-sphingomyelin substrate was prepared by drying under N_2 gas and rehydrating with assay buffer to a final concentration of 250 μg/ml. SPH standards or culture supernatants (50 μl) were incubated with 150 μl of TNPAL-sphingomyelin at 25°C for 5 min. Reactions were stopped by adding 750 μl of isopropanol–heptane–5 M H_2SO_4 (40:10:1 [vol/vol/vol]) to each reaction mixture. Heptane (450 μl) and H_2O (400 μl) were added to each reaction mixture, and after thorough mixing and centrifugation for 5 min at 2,200 × *g*, the OD_{340} of the upper, heptane-rich phase (200 μl) was determined. SPH concentrations in culture supernatants were extrapolated from the *B. cereus* SPH standard curve. Each sample and standard were assayed in triplicate. The CAMP test was also used to analyze SPH activities of each strain following 18 h of incubation at 37°C (5).

(vi) Motility. Relative swarming of *B. thuringiensis* strains was analyzed on motility agar (Difco). Colony diameters were measured after 18 h of incubation at 37°C.

Experimental *Bacillus* endophthalmitis. Experimental *B. thuringiensis* endophthalmitis was induced in New Zealand White rabbits as previously described (8, 11). The animals were maintained in accordance with institutional animal care guidelines and the Association for Research in Vision and Ophthalmology Statement on the Use of Laboratory Animals in Ophthalmic Research (3). The rabbits were anesthetized with a mixture of ketamine (Ketaved [Phoenix Scientific Inc., St. Joseph, Mo.], 35 mg/kg of body weight) and xylazine (Rompun [Bayer Corp., Shawnee Mission, Kans.]; 5 mg/kg of body weight). Topical anesthetic (0.5% proparacaine HCl [Ophthetic Allergan, Hormigueros, Puerto Rico]) was applied before each surgical procedure. A 100-μl volume of aqueous humor was withdrawn prior to each intravitreal injection by paracentesis. Then 100 CFU of *B. thuringiensis* was delivered by slow infusion into the midvitreous via a 30-gauge needle attached to a 1-ml syringe introduced through the pars plana. The contralateral eye was injected with BHI (surgical control) or was left undisturbed (absolute control). At various times postinjection, infection courses were analyzed by biomicroscopy, electroretinography (ERG), histopathology, and bacterial and inflammatory cell quantification as described below.

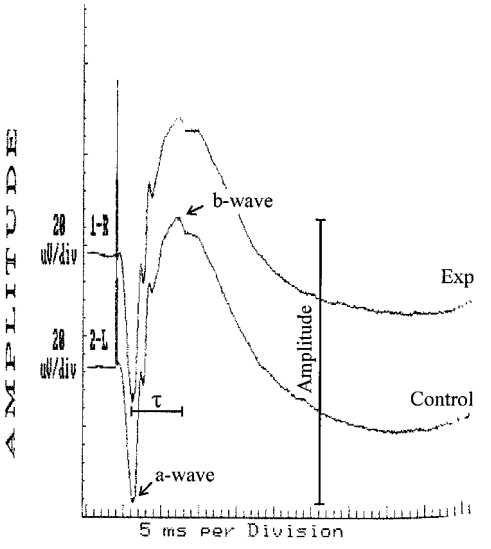

FIG. 1. Representative ERG waveform. This waveform was obtained 6 h following intravitreal injection of saline (Exp). The control eye was left undisturbed (Control). Retinal-function analyses included measurement of the amplitude and implicit time (τ) from a-wave to b-wave peaks of each waveform, as indicated.

Biomicroscopy. Rabbits were observed with a Topcon SL-5D slit-lamp biomicroscope (Kogaku Kikai K.K., Tokyo, Japan) prior to and at 6, 12, and 18 h following intravitreal injection.

Retinal function analysis. Retinal function was measured by ERG as previously described (8, 11). After dilation and 30 min of dark adaptation, b-wave responses to single light flashes (1/s) were measured (Fig. 1). b-wave amplitudes were recorded for each eye before and at various times postinjection, using scotopic bright-flash ERG (EPIC2000 [LKC Technologies, Inc., Gaithersburg, Md.]). b-wave responses for each time point represented the average of 14 repeated measures. The percent retinal function retained was calculated as 100 − ([1 − (experimental b-wave amplitude/control b-wave amplitude)] × 100) (8, 11). The percent increase in implicit time (τ) from the a-wave valley to the b-wave peak (latency) was calculated as $[1 - (\tau_{experimental}/\tau_{control})] \times 100$ (Fig. 1).

Bacterial enumeration. Enumeration of organisms in ocular tissues has been previously described (8, 11). Briefly, globes were enucleated and the vitreous removed and homogenized. Bacteria in the vitreous were quantified by track plating serial 10-fold dilutions onto BHI (21). Retention of mutant phenotypes was confirmed by phenotypic assays of bacteria recovered from the eyes.

Anterior-segment inflammation. Aqueous humor samples (approximately 100 μl per eye) were recovered by paracentesis. Infiltrating inflammatory cells in 10-μl aliquots were stained with 0.4% trypan blue and enumerated using a hemocytometer.

Thin-section histology. Globes recovered for histological analysis were fixed in 10% formalin for 24 h. The eyes were sectioned and stained with hematoxylin and eosin by standard procedures (42).

Statistical analysis. Values for parameters used to analyze progressive infection represented the mean ± standard error of the mean (SEM) for at least four eyes per time point, unless otherwise specified. Wilcoxon's rank sum test was used for statistical comparison between infection groups unless otherwise specified. $P \leq 0.05$ was considered significant.

RESULTS

***B. thuringiensis* isogenic mutants.** Transformation of strain BT407 with plasmids containing *plcA* or *plcB* each disrupted with *lacZ* yielded isogenic insertional mutants that were Lac^+ on X-Gal agar and were erythromycin sensitive, indicating a double-crossover recombination event. PCR analysis of *plcA* in strain BT407 produced the predicted 1.7-kb fragment. PCR

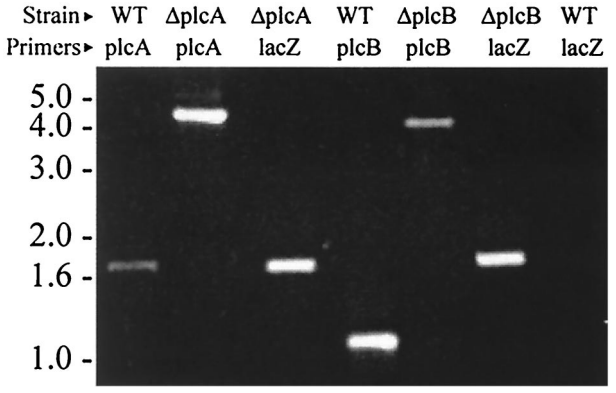

FIG. 2. PCR analysis of *B. thuringiensis* wild type and isogenic mutants. Chromosomal DNA from wild-type strain BT407 and mutant strains BT*plcA*::*lacZ* (ΔplcA), and BT*plcB*::*lacZ* (ΔplcB), were used to amplify *plcA*, *plcB*, or *lacZ*, as indicated in the figure. PCR products were of the predicted sizes (indicated by molecular weights [in thousands] on the left).

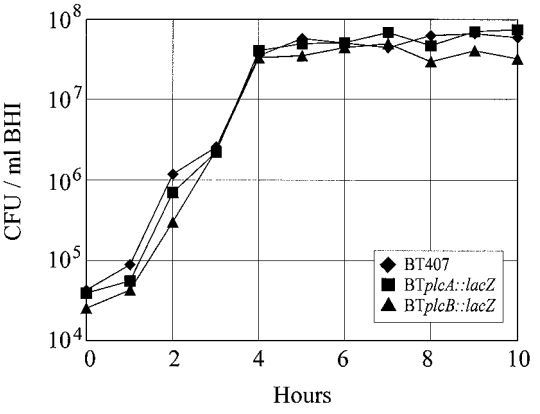

FIG. 3. In vitro growth of *B. thuringiensis* wild type and isogenic mutants. Bacteria were quantified hourly throughout 10 h of growth in BHI. The strains analyzed were wild-type strain BT407, BT*plcA*::*lacZ*, and BT*plcB*::*lacZ*.

analysis of *plcA* in strain BT*plcA*::*lacZ* produced the predicted 4.7-kb fragment due to the insertion of the 3.2-kb *lacZ* fragment between *plcA* fragments of 0.8 kb (PlcA1-PlcA2 product) and 0.7 kb (PlcA3 and PlcA4 product). PCR analysis of *plcB* in strain BT407 producted the predicted 1.1-kb fragment. PCR analysis of *plcB* in strain BT*plcB*::*lacZ* produced the predicted 4.3-kb fragment due to the insertion of the 3.2-kb *lacZ* fragment between *plcB* fragments of 0.6 kb (PlcB1-PlcB2 product) and 0.5 kb (PlcB3-PlcB4 product). PCR analysis using *lacZ*-specific primers confirmed the presence of the 1.7-kb *lacZ* fragment in the mutant strains but not in strain BT407 (Fig. 2). Additional verification of the integration of *lacZ* into *plcA* or *plcB* was carried out by PCR using upstream primers external to the *plcA* and *plcB* fragments used in strain constructions and a primer located near the 5′ end of *lacZ*. Fragments of 1.3 kb were detected following amplification of chromosomal DNA from each mutant but not from wild-type strain BT407, as anticipated (data not shown).

Results of the phenotypic assessment of strains BT407, BT*plcA*::*lacZ* and BT*plcB*::*lacZ* are summarized in Table 3. Strains BT*plcA*::*lacZ* and BT*plcB*::*lacZ* differed from wild-type strain BT407 in the disrupted gene product of interest, as measured by chromogenic and agar well diffusion assays specifically for PI-PLC and PC-PLC, respectively. The hemolytic and proteolytic activities of all strains were equivalent throughout 18 h of in vitro growth, and all strains were motile (Table 3). The in vitro growth of all strains over a 10-h period was also similar (Fig. 3).

Experimental *B. thuringiensis* endophthalmitis. Reproducible *B. thuringiensis* endophthalmitis was achieved by intravitreal injection of 1.99 ± 0.06 $\log_{10}$ CFU of strain BT407. Whole-organ and retinal histology and representative ERG waveforms of progressive endophthalmitis are depicted in Fig. 4. A mild posterior-segment inflammatory response began as early as 6 h. Mild conjunctival inflammation and 5 to 10 inflammatory cells per microscope field were present in the anterior chamber. At 6 h, all eyes had a normal fundus reflex. At 12 h postinfection, inflammatory changes in the posterior segment and anterior chamber progressed. A haze developed in the vitreous, and the fundus reflex was diminished in all eyes. From 12 to 18 h, inflammatory symptoms were severe in all

TABLE 3. Phenotypic analysis of *B. thuringiensis* BT407 and its isogenic mutants BT*plcA*::*lacZ* and BT*plcB*::*lacZ*

Strain	Hemolytic titer[a]		Phenotypic assay				
	Log phase	Stationary phase	PI-PLC[b] (μg/ml)	PC-PLC[c] (μg/ml)	SPH[e]	Protease[f] (U/ml)	Motility[g] (mm)
BT407	64	128	12.9 ± 0.2	1.7 ± 0.4	ND	6.1 ± 1.6	61.5 ± 0.9
BT*plcA*::*lacZ*	64	128	1.6 ± 0.6	2.3 ± 0.2	ND	4.2 ± 1.3	62.8 ± 0.8
BT*plcB*::*lacZ*	64	128	13.3 ± 0.1	ND[d]	ND	4.9 ± 2.0	76.0 ± 2.2

[a] Hemolytic assay of filtered supernatants of 8-h (logarithmic phase) and 18-h (stationary phase) *B. thuringiensis* cultures. A twofold difference in titer was considered significant.

[b] Chromogenic PI-PLC assay. Values represent mean ± standard deviation in filtered supernatants of 10-h *B. thuringiensis* cultures. PI-PLC activity in strain BT*plcA*::*lacZ* supernatants was significantly lower than in other strains ($P \leq 0.002$, Student's *t* test) but similar to that in heat-denatured controls ($P \geq 0.433$, Student's *t* test).

[c] Egg yolk agar well diffusion assay for PC-PLC activity. Values represent mean ± standard deviation in filtered supernatants of 8-h *B. thuringiensis* cultures. Values for BT407 and BT*plcA*::*lacZ* were not significantly different ($P \geq 0.06$, Student's *t* test).

[d] ND, not detected.

[e] Chromogenic SPH assay and CAMP test. No SPH activity was detected in filtered supernatants of 4-, 8-, 10-, 12-, and 18-h *B. thuringiensis* cultures. Negative CAMP reactions were also observed.

[f] Hide azure blue protease assay. Values represent mean ± standard deviation in filtered supernatants of 10-h *B. thuringiensis* cultures. Values were not significantly different ($P \geq 0.08$, Student's *t* test).

[g] Swarming on motility agar. Values represent mean diameter ± standard deviation after an 8-h incubation at 37°C. Diameters of BT*plcB*::*lacZ* colonies were significantly larger than that of the other groups at 18 h ($P \leq 0.001$, Student's *t* test).

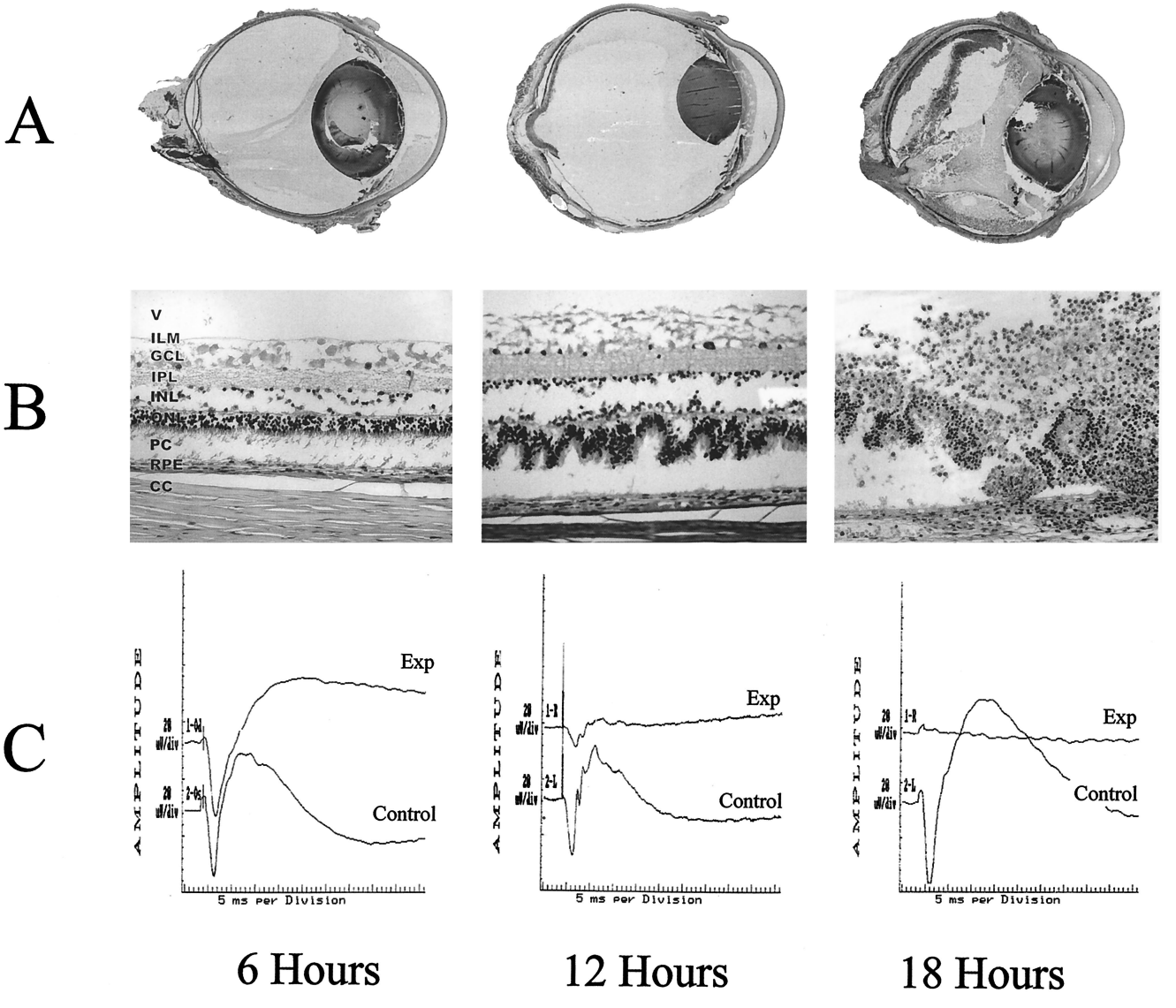

FIG. 4. Histologic and ERG analysis of progressive experimental *B. thuringiensis* endophthalmitis. Whole-organ (A) and retinal (B) histology of eyes intravitreally injected with approximately 2 $\log_{10}$ of strain BT407 at 6, 12, and 18 h postinfection are shown. (Panel A reprinted from reference 11a with permission of the publisher.) All representative histologic sections were stained with hematoxylin and eosin. In whole-organ sections, severe inflammation and retinal detachment were observed by 18 h. Photoreceptor folding was observed in retinal sections by 12 h. By 18 h, retinal layers were difficult to differentiate. Abbreviations: V, vitreous; ILM, inner limiting membrane; GCL, ganglion cell layer; IPL, inner plexiform layer; INL, inner nuclear layer; ONL, outer nuclear layer; PC, photoreceptor cell layer; RPE, retinal pigment epithelium; CC, choriocapillaris. Magnifications, ×8 (A) and ×160 (B). (C) Representative ERG waveforms obtained at 6, 12, and 18 h following intravitreal injection of strain BT407 (Exp). Control eyes were left undisturbed (Control). Sharp decreases in b-wave amplitude were observed in infected eyes at 12 h. b-wave responses were virtually absent in infected eyes by 18 h.

eyes, with severe iritis, significant inflammatory-cell infiltration into the vitreous and cornea, and no fundus reflex. By 18 h, corneal ring infiltrates were present in at least one-third of eyes in each infection group. Severe inflammation of periorbital tissues was also present in all eyes. Because of the impending panophthalmitis at this time point, infections were not allowed to progress further. No pathologic changes were observed in surgical or absolute controls 6, 12, and 18 h postinfection.

Experimental PI-PLC- and PC-PLC-deficient *B. thuringiensis* endophthalmitis. The in vivo growth of *B. thuringiensis* strains is summarized in Fig. 5A. Intraocular numbers of strain BT*plcA*::*lacZ* were significantly smaller at 6 and 12 h than were those of strain BT407 ($P \leq 0.01$) but were similar to those of strain BT407 at 18 h ($P = 0.79$). Intraocular growth patterns of strains BT407 and BT*plcB*::*lacZ* were similar at each time point assayed ($P \geq 0.08$). In general, each strain grew logarithmically until approximately 6 h, after which a stationary phase of growth was maintained until the termination of the experiment. Gross inflammatory changes observed in eyes infected with strains BT*plcA*::*lacZ* or BT *plcB*::*lacZ* were similar to those observed in eyes infected with wild-type strain BT407 at all time points throughout the infection courses.

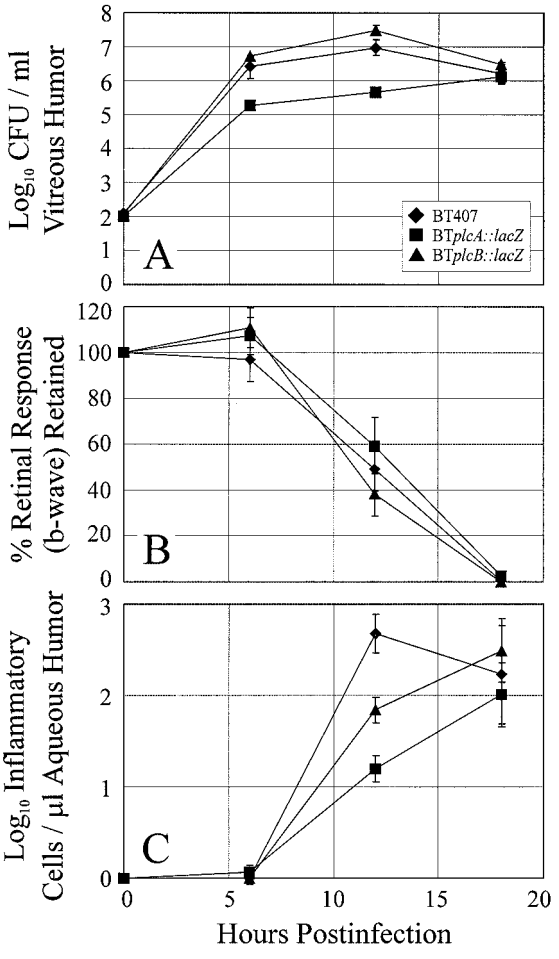

FIG. 5. Comparison of experimental *B. thuringiensis* endophthalmitis initiated by wild-type and isogenic mutant strains. Inocula of approximately 2 $\log_{10}$ of either strain BT407, BT*plcA*::*lacZ*, or BT*plcB*::*lacZ* were injected intravitreally, and infectious were analyzed by bacterial enumeration (A), ERG (B), and inflammatory cell quantitation (C). All values represent the mean and SEM for at least four eyes per group.

Retinal function analyses. Retinal function analyses of eyes infected with *B. thuringiensis* wild-type and mutant strains are summarized in Fig. 5B. The b-wave amplitudes of surgical and absolute control eyes remained at preoperative levels throughout the duration of the experiment (data not shown). The b-wave amplitudes of eyes infected with strain BT407 were similar to preoperative levels and to control eyes at 6 h ($P \geq 0.88$) but retained only 48.9% ± 9.2% responsiveness by 12 h. At 18 h, retinal responses were nearly absent (retinal function retained = 0.41% ± 0.33%).

The b-wave amplitudes of eyes injected with strains BT*plcA*::*lacZ* or BT*plcB*::*lacZ* were similar to preoperative levels and to those of controls and strain BT407 at 6 h ($P \geq 0.33$). At 12 and 18 h, b-wave amplitudes in eyes infected with each mutant were similar to that of strain BT407 ($P \geq 0.19$). By 18 h, b-wave responses in eyes infected with each mutant strain were essentially absent (Fig. 5B).

Representative waveforms showing implicit time values (τ) from ERG responses are shown in Fig. 6. τ values for eyes infected with strain BT407 were increased by 383% ± 68% compared to controls at 6 h ($P = 0.0001$). τ values for eyes infected with strains BT*plcA*::*lacZ* or BT*plcB*::*lacZ* were not increased above that of controls at 6 h ($P \geq 0.85$). τ values for all infection groups were similar to those of controls at 12 and 18 h ($P \geq 0.25$, data not shown).

Anterior-segment inflammation. Enumeration of inflammatory cells in aspirated aqueous humor samples is summarized in Fig. 5C. Few inflammatory cells were recovered from infected eyes at 6 h. By 12 h, significantly larger numbers of inflammatory cells were recovered from strain BT407-infected eyes than from eyes infected with each mutant strain ($P \leq 0.03$). By 18 h, the numbers of inflammatory cells recovered from eyes infected with each mutant strain increased and were similar to those recovered from eyes infected with BT407 ($P \geq 0.73$).

Histology. Whole-organ and retinal histologic analysis of progressive *B. thuringiensis* endophthalmitis is summarized in Fig. 7. Immediately following intravitreal injection, eyes from all infection groups possessed intact retinal architecture, no observable inflammation, and few bacilli in the vitreous (data not shown). At 6 h, eyes injected with wild-type strain BT407 and each mutant exhibited a mild inflammatory response in the posterior segment that originated from the optic nerve head and the ciliary body. The retinal architecture of all infected eyes was intact, and bacilli were observed throughout the vitreous, primarily within vitreous structures. Few inflammatory cells were observed in the anterior segment, and the corneas appeared normal. By 12 h, significant inflammation was observed in all eyes, with large numbers of inflammatory cells and fibrin seen in the posterior and anterior segments. Distinct folding of retinal layers and partial retinal detachments were also observed. Bacilli could be seen in both the posterior and anterior segments of the majority of infected eyes at 12 h. By 18 h, complete retinal tissue dissolution, significant edema, and chemosis of all ocular and surrounding periocular tissues and inflammatory cells in all parts of the eye and surrounding tissues were observed. Histologic specimens from eyes infected with strain BT407 or each mutant were indistinguishable at each time point throughout infection (Fig. 7).

DISCUSSION

B. cereus, *B. thuringiensis*, and *B. anthracis* are members of the *B. cereus* group, a taxonomic group demonstrating similar genetic profiles, as demonstrated by multilocus enzyme electrophoresis comparing a number of chromosomal genes in these strains (18). The key difference between *B. thuringiensis* and *B. cereus* is the presence of genes coding for insectidical (*cry*) toxins in *B. thuringiensis*. If these *cry* plasmids are lost, as is the case with the strains used in these studies, *B. thuringiensis* and *B. cereus* are essentially indistinguishable. Both species are motile and produce a plethora of hemolysins, enterotoxins, and proteases, all of which are possible virulence factors that may contribute to the pathogenesis of disease.

Because of the genetic and phenotypic similarities between *B. cereus* and *B. thuringiensis*, we used a well-characterized strain of *B. thuringiensis* in our model of experimental endophthalmitis (8, 11). Experimental *B. thuringiensis* endophthalmitis resulted in extensive inflammation and loss of retinal function

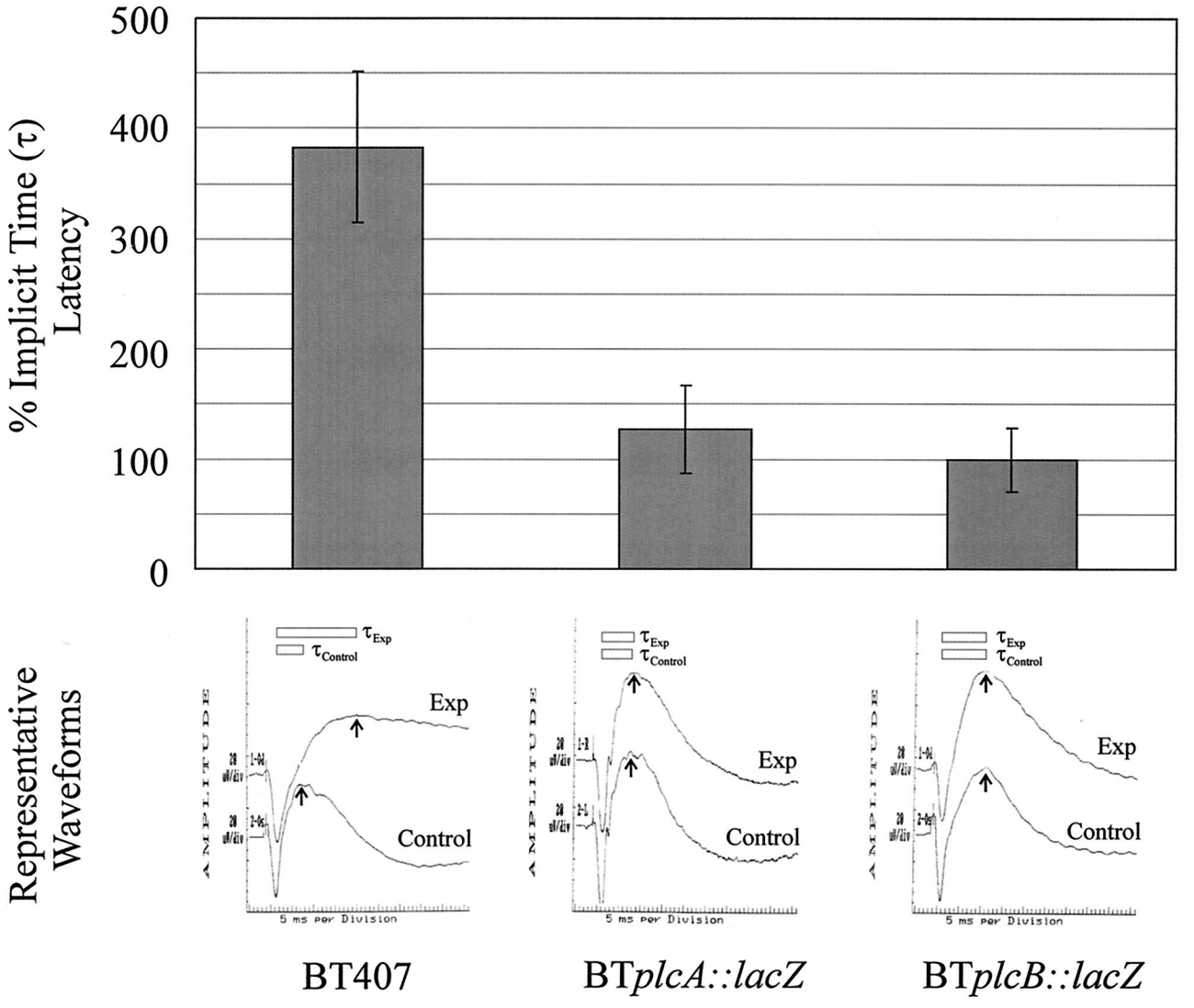

FIG. 6. Analysis of latent b-wave responses in experimental *B. thuringiensis* endophthalmitis. The percent implicit time (τ) from a-wave valleys to b-wave peaks and representative waveforms from eyes intravitreally injected with strains BT407, BT*plcA*::*lacZ*, and BT*plcB*::*lacZ* at 6 h postinfection are shown. All values represent the mean and SEM for at least four eyes per group.

in a manner similar to that of experimental *B. cereus* endophthalmitis but at a slightly lower rate compared to a clinical isolate of *B. cereus* that caused a highly destructive endophthalmitis (8, 11). We previously reported that experimental *B. cereus* endophthalmitis abolished retinal function by 12 h (8). Extensive inflammation, complete loss of retinal function, and a severe panophthalmitis occurred with either organism within 1 day of infection with as few as 100 organisms.

The contributions of PI-PLC and PC-PLC to endophthalmitis pathogenesis were analyzed using isogenic mutants with *lacZ* insertions disrupting each gene of interest. Endophthalmitis caused by these mutant strains resulted in complete or nearly complete destruction of retinal function by 18 h, irrespective of the mutation present. Comparable levels of inflammation and retinal photoreceptor layer detachment, folding, and dissolution occurred regardless of the strain used. As in our previous finding of the limited role of hemolysin BL in *B. cereus* endophthalmitis, our results demonstrated that neither PI-PLC nor PC-PLC contributed to *B. thuringiensis* endophthalmitis pathogenesis.

An unexpected finding was the increased latency of b-wave response without loss of b-wave amplitude at 6 h in eyes infected with wild-type strain BT407 but not in eyes infected with BT*plcA*::*lacZ* or BT*plcB*::*lacZ* strains. Latent b-wave responses mark the initial events in retinal dysfunction and have been shown to occur in the early stages of degenerative retinal syndromes including diabetic retinopathy (7, 40), retinitis pigmentosa (19), and retinal ischemia (6). b-wave function results from the flow of current from the photoreceptor cell layers of the retina into the vitreous via the Müller cell in response to a visual stimulus (33). The Müller cell, which spans the length of the retina, provides architectural support and regulates neurotransmitter levels in the retina by degrading or removing these substances during neuronal activity (36). Müller cells also

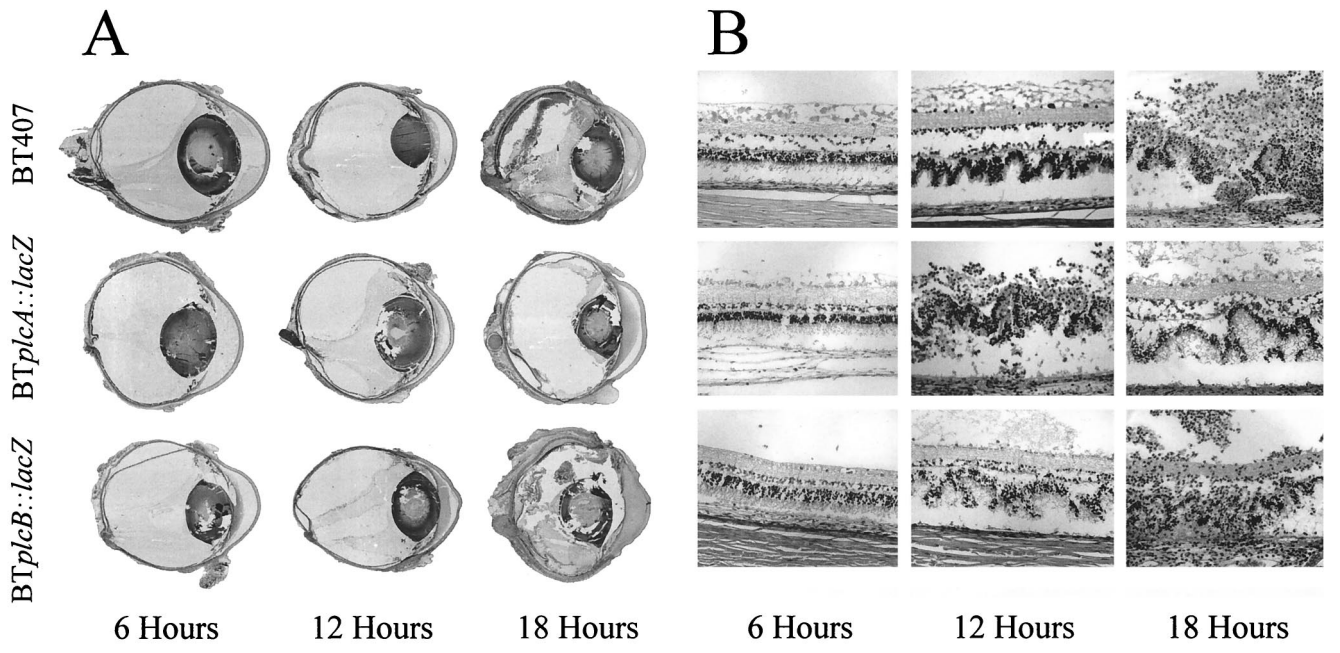

FIG. 7. Histologic analysis of experimental *B. thuringiensis* endophthalmitis. Representative whole-organ (A) and retinal (B) histology of eyes intravitreally injected with strains BT407, BT*plcA*::*lacZ*, and BT*plcB*::*lacZ* at 6, 12, and 18 h postinfection are shown. All histologic sections were stained with hematoxylin and eosin. In whole-organ sections, severe inflammation and retinal detachment were observed by 18 h. Photoreceptor folding and detachment were observed in retinal sections by 12 h. By 18 h, retinal layers were virtually indistinguishable. Gross pathologic changes observed in all infection groups were similar at all time points. Magnifications, ×9 (A) and ×180 (B). (Top row of panel A is reprinted from reference 11a with permission of the publisher.)

maintain homeostasis of potassium (K^+) levels in the retina by removing K^+ from the outer retina (31). K^+ siphoning from the photoreceptor cell layers of the retina into the vitreous during light stimulation is, in large part, the basis for the b-wave response (32). Therefore, a delayed b-wave response in this case may mark the beginnings of Müller cell dysfunction in response to infection. In endophthalmitis, retinal layers are irreversibly damaged and ultimately disrupted, but the exact mechanisms of damage to Müller cells or other retinal cell types are not known. Further analysis of the early stages of infection is needed to determine when these effects begin, what cell types are affected, and what toxins or inflammatory mediators are involved in this initial damage.

ACKNOWLEDGMENTS

We thank Sonia Senesi, Emilia Ghelardi (Dipartimento di Patologia Sperimentale, Universita di Pisa, Pisa, Italy), and Doug Beecher (Hazardous Materials Response Unit, FBI Academy, Quantico, Va.) for sharing BT407 and BT*plcA*::*lacZ* strains, and we thank Wei Cao (University of Oklahoma Health Sciences Center, Oklahoma City, Okla.) for stimulating discussions. The technical assistance of Mark Dittmar (DMEI Animal Facility, Oklahoma City, Okla.) and Paula Pierce (DMEI Pathology Laboratory, Oklahoma City, Okla.) is also greatly appreciated.

This work was supported by the National Institutes of Health (EY12985), by Fight for Sight/Prevent Blindness America, and by an unrestricted Career Development Award from Research to Prevent Blindness, Inc. (M.C.C.).

REFERENCES

1. **Agaisse, H., and D. Lereclus.** 1994. Structural and functional analysis of the promoter region involved in full expression of the *cryIIIA* toxin gene of *Bacillus thuringiensis*. Mol. Microbiol. **13:**97–107.
2. **Alape-Giron, A., M. Flores-Diaz, I. Guillouard, C. E. Naylor, R. W. Titball, A. Rucavado, B. Lomonte, A. K. Basak, J. M. Gutierrez, S. T. Cole, and M. Thelestam.** 2000. Identification of residues critical for toxicity in *Clostridium perfringens* phospholipase C, the key toxin in gas gangrene. Eur. J. Biochem. **267:**5191–5197.
3. **Association for Research in Vision and Ophthalmology.** 2000. Statement for the use of animals in ophthalmic and visual research. [Online.] http://www.arvo.org/animalst.htm. Association for Research in Vision and Ophthalmology, Hagerstown, Md.
4. **Beecher, D. J., T. W. Olsen, E. B. Somers, and A. C. Wong.** 2000. Evidence for contribution of tripartite hemolysin BL, phosphatidylcholine-preferring phospholipase C, and collagenase to virulence of *Bacillus cereus* endophthalmitis. Infect. Immun. **68:**5269–5276.
5. **Bernheimer, A. W., R. Linder, and L. S. Avigad.** 1979. Nature and mechanism of action of the CAMP protein of group B streptococci. Infect. Immun. **3:**838–844.
6. **Block, F., and M. Schwarz.** 1998. The b-wave of the electroretinogram as an index of retinal ischemia. Gen. Pharmacol. **30:**281–287.
7. **Bresnick, G. H., and M. Palta.** 1987. Temporal aspects of the electroretinogram in diabetic retinopathy. Arch. Ophthalmol. **105:**660–664.
8. **Callegan, M. C., M. C. Booth, B. D. Jett, and M. S. Gilmore.** 1999. Pathogenesis of gram-positive bacterial endophthalmitis. Infect. Immun. **67:**3348–3356.
9. **Callegan, M. C., L. S. Engel, J. M. Hill, and R. J. O'Callaghan.** 1994. Corneal virulence of *Staphylococcus aureus*: roles of alpha-toxin and protein A in pathogenesis. Infect. Immun.**62:**2478–2482.
10. **Callegan, M. C., M. Engelbert, D. W. Parke, and B. D. Jett, M. S. Gilmore.** 2002. Bacterial endophthalmitis: epidemiology, therapeutics, and bacterium-host interactions. Clin. Microbiol. Rev. **15:**111–124.
11. **Callegan, M. C., B. D. Jett, L. E. Hancock, and M. S. Gilmore.** 1999. Role of hemolysin BL in the pathogenesis of extraintestinal *Bacillus cereus* infection as assessed using an endophthalmitis model. Infect. Immun. **67:**3357–3366.

11a. **Callegan, M. C., S. T. Kane, D. C. Cochran, and M. S. Gilmore.** 2002. Molecular mechanisms of *Bacillus* endophthalmitis pathogenesis. DNA Cell Biol. **21:**367–373.

12. **Daugherty, S., and M. G. Low.** 1993. Cloning, expression, and mutagenesis of phosphatidylinositol-specific phospholipase C from *Staphylococcus aureus*: a potential staphylococcal virulence factor. Infect. Immun. **61:**5078–5089.
13. **Gatt S., T. Dinur, and Y. Barenholz.** 1978. A spectrophotometric method for determination of sphingomyelinase. Biochim. Biophys. Acta **530:**503–507.
14. **Gilmore, M. S., M. C. Callegan, and B. D. Jett.** 1999. Multicomponent

cytolysins of *Enterococcus faecalis* and *Bacillus cereus*, p. 419–434. *In* J. E. Alouf and J. H. Freer (ed.), Comprehensive sourcebook: bacterial protein toxins. Academic Press, Ltd., London, United Kingdom.
15. **Gilmore M. S., A. M. Cruz-Rodz, M. Leimeister-Wächter, J. Kreft, and W. Goebel.** 1989. A *Bacillus cereus* cytolytic determinant, cereolysin AB, which comprises the phospholipase C and sphingomyelinase genes: nucleotide sequence and genetic linkage. J. Bacteriol. **171:**744–753.
16. **Gominet, M., L. Slamti, N. Gilois, M. Rose, and D. Lereclus.** 2001. Oligopeptide permease is required for expression of the *Bacillus thuringiensis plcR* regulon and for virulence. Mol. Microbiol. **40:**963–975.
17. **Grassme, H., V. Jendrossek, and E. Gulbins.** 2001. Molecular mechanisms of bacteria induced apoptosis. Apoptosis **6:**441–445.
18. **Helgason, E., O. A. Okstad, D. A. Caugant, H. A. Johansen, A. Fouet, M. Mock, I. Hegna, and A. B. Kolsto.** 2000. *Bacillus anthracis*, *Bacillus cereus*, and *Bacillus thuringiensis*: one species on the basis of genetic evidence. Appl. Environ. Microbiol. **66:**2627–2630.
19. **Iijima H., S. Yamaguchi, and O. Hosaka.** 1993. Photopic electroretinogram implicit time in retinitis pigmentosa. Jpn. J. Ophthalmol. **37:**130–135.
20. **Ikezawa, H., and R. Taguchi.** 1981. Phosphatidylinositol-specific phospholipase C from *Bacillus cereus* and *Bacillus thuringiensis*. Methods Enzymol. **71:**731–741.
21. **Jett, B. D., K. L. Hatter, M. M. Huycke, and M. S. Gilmore.** 1997. Simplified agar plate method for quantifying viable bacteria. BioTechniques **23:**648–650.
22. **Jett, B. D., H. G. Jensen, R. E. Nordquist, and M. S. Gilmore.** 1992. Contribution of the pAD1-encoded cytolysin to the severity of experimental *Enterococcus faecalis* endophthalmitis. Infect. Immun. **60:**2445–2452.
23. **Johansen, T., T. Holm, P. H. Guddal, K. Sletten, F. B. Haugli, and C. Little.** 1988. Cloning and sequencing of the gene encoding the phosphatidylcholine-preferring phospholipase C of *Bacillus cereus*. Gene **65:**293–304.
24. **Kuppe, A., L. M. Evans, D. A. McMillan, and O. H. Griffith.** 1989. Phosphatidylinositol-specific phospholipase C of *Bacillus cereus*: cloning, sequencing, and relationship to other phospholipases. J. Bacteriol. **171:**6077–6083.
25. **Lereclus, D., H. Agaisse, M. Gominet, and J. Chaufaux.** 1995. Overproduction of encapsulated insecticidal crystal proteins in a *Bacillus thuringiensis spo0A* mutant. Bio/Technology **13:**67–71.
26. **Lereclus, D., H. Agaisse, M. Gominet, S. Salamitou, and V. Sanchis.** 1996. Identification of a *Bacillus thuringiensis* gene that positively regulates transcription of the phosphatidylinositol-specific phospholipase C gene at the onset of the stationary phase. J. Bacteriol. **178:**2749–2756.
27. **Lereclus, D., O. Arantes, J. Chaufaux, and M. M. Lecadet.** 1989. Transformation and expression of a cloned δ-endotoxin gene in *Bacillus thuringiensis*. FEMS Microbiol. Lett. **60:**211–217.
28. **Lereclus, D., M. Vallade, J. Chaufaux, O. Arantes, and S. Rambaud.** 1992. Expansion of insecticidal host range of *Bacillus thuringiensis* by *in vivo* genetic recombination. Bio/Technology **10:**418–421.
29. **Marques, M. B., P. F. Weller, J. Parsonnet, B. J. Ransil, and A. Nicholson-Weller.** 1989. Phosphatidylinositol-specific phospholipase C, a possible virulence factor of *Staphylococcus aureus*. Infect. Immun. **27:**2451–2454.
30. **Msadek, T., F. Kunst, D. Henner, A. Klier, G. Rapoport, and R. Dedonder.** 1990. Signal transduction pathway controlling synthesis of a class of degradative enzymes in *Bacillus subtilis*: expression of the regulatory genes and analysis of mutations in *degS* and *degU*. J. Bacteriol. **172:**824–834.
31. **Newman, E. A.** 1985. Regulation of extracellular potassium by glial cells in the retina. Trends Neurosci. **8:**156–159.
32. **Newman, E. A., D. A. Frambach, and L. L. Odette.** 1984. Control of extracellular potassium levels by retinal glial cell K^+ siphoning. Science **225:**1174–1175.
33. **Newman, E. A., and L. L. Odette.** 1984. Model of electroretinogram b-wave generation: a test of the K^+ hypothesis. J. Neurophysiol. **51:**164–182.
34. **Ng, E. W., N. Samiy, J. B. Rubins, F. V. Cousins, K. L. Ruoff, A. S. Baker, and D. J. D'Amico.** 1997. Implication of pneumolysin as a virulence factor in *Streptococcus pneumoniae* endophthalmitis. Retina **17:**521–529.
35. **O'Callaghan, R. J., M. C. Callegan, J. M. Moreau, L. C. Green, T. J. Foster, O. M. Hartford, L. S. Engel, and J. M. Hill.** 1997. Specific roles of alpha-toxin and beta-toxin during *Staphylococcus aureus* corneal infection. Infect. Immun. **65:**1571–1578.
36. **Reichenbach A., and S. R. Robinson.** 1995. The involvement of Müller cells in the outer retina, p. 395–416. *In* M. B. A. Djamgoz, S. N. Archer, and S. Vallerga (ed.), Neurobiology and Clinical aspects of the outer retina. Chapman & Hall, London, United Kingdom.
37. **Rinderknecht, H., M. C. Geokas, P. Silverman, and B. J. Haverback.** 1968. A new ultrasensitive method for the determination of proteolytic activity. Clin. Chim. Acta **21:**197–203.
38. **Rose, F., S. A. Zeller, T. Chakraborty, E. Domann, T. Machleidt, M. Kronke, W. Seeger, F. Grimminger, and U. Sibelius.** 2001. Human endothelial cell activation and mediator release in response to *Listeria monocytogenes* virulence factors. Infect. Immun. **69:**897–905.
39. **Saint-Joanis, B., T. Garnier, and S. T. Cole.** 1989. Gene cloning shows the alpha-toxin of *Clostridium perfringens* to contain both sphingomyelinase and lecithinase activities. Mol. Gen. Genet. **219:**453–460.
40. **Satoh, S., H. Iijima, M. Imai, K. Abe, and T. Shibuya.** 1994. Photopic electroretinogram implicit time in diabetic retinopathy. Jpn. J. Ophthalmol. **38:**178–184.
41. **Schluter, D., E. Domann, C. Buck, T. Hain, H. Hof, T. Chakraborty, and M. Deckert-Schluter.** 1998. Phosphatidylcholine-specific phospholipase C from *Listeria monocytogenes* is an important virulence factor in murine cerebral listeriosis. Infect. Immun. **66:**5930–5938.
42. **Sheehan, D. C., and B. B. Hrapchak.** 1987. Theory and practice of histotechnology. Batelle Press, Columbus, Ohio.
43. **Sibelius, U., E. C. Schulz, F. Rose, K. Hattar, T. Jacobs, S. Weiss, T. Chakraborty, W. Seeger, and F. Grimminger.** 1999. Role of *Listeria monocytogenes* exotoxins listeriolysin and phosphatidylinositol-specific phospholipase C in activation of human neutrophils. Infect. Immun. **67:**1125–1130.
44. **Villafane, R., D. H. Bechhofer C. S. Narayanan, and D. Dubnau.** 1987. Replication control genes of plasmid pE194. J. Bacteriol. **169:**4822–4829.
45. **Zhang, P., B. Liu, G. M. Jenkins, Y. A. Hannun, and L. M. Obeid.** 1997. Expression of neutral sphingomyelinase identifies a distinct pool of sphingomyelin involved in apoptosis. J. Biol. Chem. **272:**9609–9612.

Editor: E. I. Tuomanen